Heat conduction in paraffin wax

Hamers, Joep; Meulendijks, Bart F.M.

Award date:
2024

Heat conduction in paraffin wax

Joep Hamers
1444344

Research group Processing and Performance (P&P)
Department of Mechanical Engineering
Technical University of Eindhoven

In collaboration with Bart Meulendijks (b.f.m.meulendijks@student.tue.nl)

Supervisors: Aricia Rinkens (a.rinkens@tue.nl)
Clemens Verhoosel (c.v.verhoosel@tue.nl)
Rodrigo Lima De Souza E Silva(r.lima.de.souza.e.silva@tue.nl)

Eindhoven, July 2, 2024

Contents

1 Theoretical Background **4**
- 1.1 Motivation . . . 4
- 1.2 Theoretical Analysis . . . 4

2 Experimental setup **6**
- 2.1 Prototype . . . 6
- 2.2 Improved Design . . . 6
- 2.3 Electric components . . . 7
  - 2.3.1 Peltier Element . . . 8
  - 2.3.2 Temperature Sensors . . . 8
  - 2.3.3 Adaptor/Temperature Controller . . . 9

3 Numerical Model **10**
- 3.1 Model Setup . . . 10
- 3.2 Boundary Conditions . . . 11
  - 3.2.1 Dirichlet Boundary Condition . . . 11
  - 3.2.2 Neumann (Convective) Boundary Condition . . . 11
- 3.3 Numerical Implementation . . . 12
- 3.4 Simulation Execution . . . 12

4 Comparison to the experiment **14**
- 4.1 Temperature Distribution . . . 14
- 4.2 Improvements and Future Work . . . 15

5 Conclusion **16**

6 Appendix A **18**

7 Appendix B **21**

List of Symbols

The table below consists of symbols, descriptions, and units for variables used in this report. If a unit is used in a specific way, other than stated in the list below, it will be mentioned.

Symbol	**Variable**	**Unit**	**Unit abbreviation**
T	Temperature	Kelvin	K
t	Time	Seconds	s
k	Thermal conductivity	Watts per meter-kelvin	$\mathrm{W/(m \cdot K)}$
L	Length	Meter	m
R	Radius	Meter	m
A	Area	Meter squared	m^2
ρ	Density	Kg per cubic meter	kg/m^3
C_p	Specific heat	Joules per kilogram kelvin	$\mathrm{J/(kg \cdot K)}$
m	Mass	Kilogram	Kg
α	Thermal Diffusivity	square meters per second	m^2/s
Q	Heat	Joule	J

Introduction

Together with the Energy Technology section, the Processing and Performance of Materials section set up the project of heat conduction in paraffin wax. The aim of this project is to solve a heat conduction problem by determining the thermal conductivity of paraffin wax. This project will involve a numerical analysis and an experimental validation. A experimental setup will be developed and experiments will be conducted to ensure the model's accuracy.

The primary goals of this Bachelor End Project (BEP) are to create an experimental setup to measure the heat conduction of paraffin wax and to validate the results with a numerical model. In collaboration with Bart Meulendijks, this project is divided into two distinct parts. This report will address the creation and validation of the numerical model that simulates the experimental conditions and results, while Bart will mainly focus on conducting the experiments and interpretation of the experimental results.

The experimental setup will be explained in detail and the model will give insights in the setup of the model as well as the different boundary conditions used.

1 Theoretical Background

In this chapter, the groundwork for the project is established by defining the problem, delving into the relevant theoretical concepts, and discussing the essential information required for the experiment. A clear understanding of thermal conductivity and heat transfer principles is fundamental for designing the heat conduction experiment.

1.1 Motivation

This experiment will utilize paraffin, a material commonly found in candle wax. Paraffin is intriguing because it significantly differs from materials like pure metals such as aluminum or steel in terms of thermal conductivity and heat distribution [1]. While metals have high and stable thermal conductivity, paraffin's thermal conductivity is relatively low and varies with temperature. This characteristic leads to different heat distribution behaviors as the material's ability to conduct heat changes with temperature. Figure 1 illustrates this effect, where the dashed line represents the temperature distribution over distance and time with a constant thermal conductivity k, and the solid line shows the distribution with temperature-dependent conductivity.

1.2 Theoretical Analysis

Heat conduction through a material can be described using Fourier's Law of Heat Conduction [2]. This law states that the rate of heat transfer through a material is proportional to the negative gradient of the temperature and the area through which the heat flows. Mathematically, it is expressed as:

$$q = -kA\frac{dT}{dx} \tag{1}$$

where q is the heat transfer rate, k is the thermal conductivity of the material, A is the cross-sectional area through which the heat flows, and $\frac{dT}{dx}$ is the temperature gradient in the direction of heat flow.

The problem can be modeled as the classic thin metal rod experiment. This experiment involves heating one end of a metal rod and measuring the temperature along its length over time. It allows the observation of heat transfer through the material and helps determine the thermal conductivity and study different boundary conditions. Figure **??** illustrates the behavior of heat transfer in this experiment.

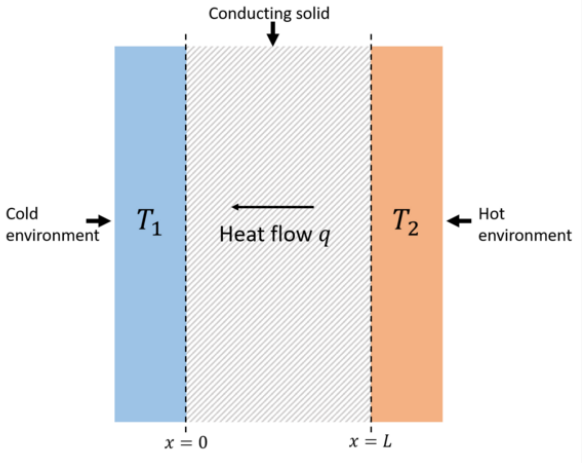

Figure 1: Constant vs Variable Thermal Conductivity k

Designing an experimental setup similar to the thin metal rod experiment to analyze heat conduction through paraffin would be beneficial.

The heat transfer in this rod can be described using the heat equation [3]. This equation describes how heat diffuses through a region in three-dimensional space over time. It is a partial differential equation given by:

$$\frac{\partial u}{\partial t} = \alpha \left(\frac{\partial^2 u}{\partial x^2} + \frac{\partial^2 u}{\partial y^2} + \frac{\partial^2 u}{\partial z^2} \right) \tag{2}$$

For simplicity, we can assume this problem to be one-dimensional. Under this assumption, the 1D heat equation for a thin metal rod experiment is:

$$\frac{\partial u(x,t)}{\partial t} = \alpha \frac{\partial^2 u(x,t)}{\partial x^2} \tag{3}$$

where $u(x,t)$ represents the temperature distribution along the rod at position x and time t. The parameter α is the thermal diffusivity of the material, defined as $\alpha = \frac{k}{\rho c}$, with k as the thermal conductivity, ρ as the density, and c as the specific heat capacity. The term $\frac{\partial u(x,t)}{\partial t}$ indicates the rate of temperature change with respect to time, while $\frac{\partial^2 u(x,t)}{\partial x^2}$ is the second spatial derivative of temperature, representing the change rate of the temperature gradient along the rod. This equation models the diffusion of heat through the rod over time.

2 Experimental setup

This chapter describes the detailed design and construction of the experimental setup, emphasizing the final result more than the construction process. The functionality of the setup is examined, highlighting key design decisions, especially regarding material choices and dimensions, while the electronic aspects are covered in detail in my colleague's report.

2.1 Prototype

The initial design comprises a cylindrical paraffin body. To ensure unidirectional heat transfer, the setup involves heating one end and actively cooling the other, with the circular surface insulated to minimize heat loss. A constant heat source is necessary, and the paraffin must be contained within an enclosed volume.

The first prototype used a large PVC tube with an 80 mm diameter and an 85 mm height. The bottom was enclosed with a thin 1 mm aluminum plate heated by a Peltier element, while the top was actively cooled using a reversed Peltier element. Two DS18B20 temperature sensors were placed at the top and bottom to measure temperatures.

This prototype demonstrated the feasibility of the setup but revealed areas for improvement:

- The aluminum heating plate was too thin to maintain a constant temperature. A thicker plate would stabilize the temperature delivery.
- The diameter could be reduced as the experiment is not dependent on the surface area, and a smaller diameter would reduce the experiment duration.
- Active cooling at the top was unnecessary.
- Two temperature sensors were insufficient to accurately measure heat distribution through the paraffin.

2.2 Improved Design

Building on insights from the prototype, the next version retained the core concept but incorporated several improvements. The key components of the updated design are illustrated in Figure **??**. An aluminum block, heated by a Peltier element with a heat sink below, delivers heat to the paraffin enclosed in a PVC tube. To maintain the aluminum block at a constant temperature, the XH-W3001 temperature controller is used. Four temperature sensors are evenly distributed throughout the paraffin to measure temperatures at specified locations, with a custom-designed sensor holder ensuring accurate placement.

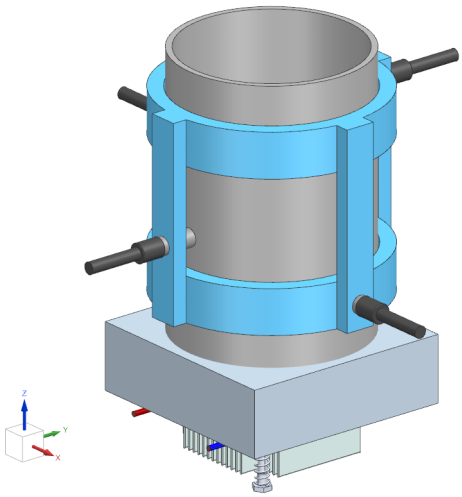

Figure 2: Core components

After determining the core components, the insulation and casing were developed. Polyurethane (PUR)

foam was selected for its low thermal conductivity of 0.028 W/m·K, much lower than PVC and paraffin. Proper casing is required due to PUR being a foam. Figures 3 and 4 show the model's section view, designed with CAD software and 3D printed to enclose the PUR, elevate the core components for easy access, and allow sensor cables to exit from the bottom. The aluminum block and PVC tube are clamped to ensure a waterproof connection.

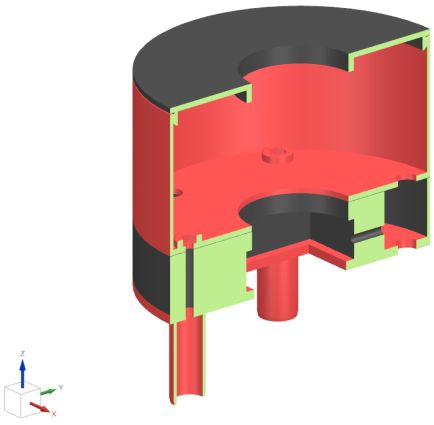

Figure 3: Cross section of casing

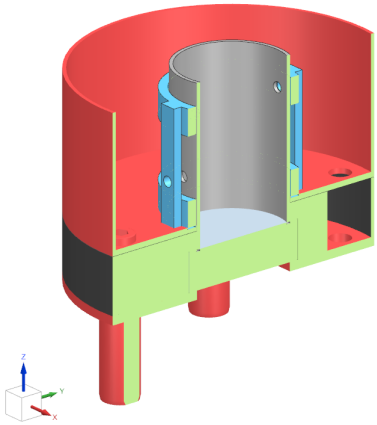

Figure 4: Cross Section of 3D model

The complete setup, shown in Figures 5 and 6, integrates all discussed components. Detailed technical drawings are available in Appendix 6.

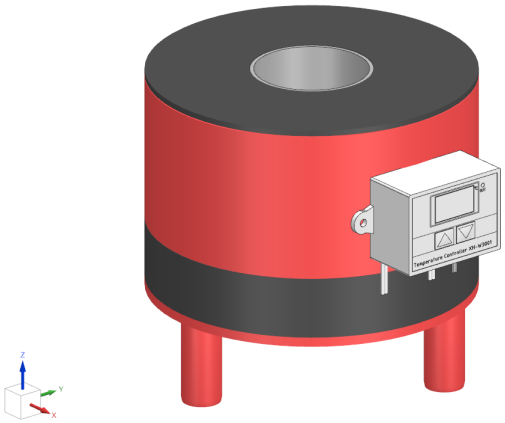

Figure 5: Complete 3D Model of the design

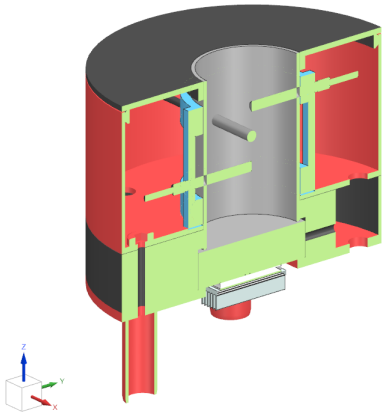

Figure 6: Cross Section of 3D model

2.3 Electric components

For data collection, the four temperature sensors are connected to an Arduino, which processes the data with a Matlab script and stores it for analysis. The sensors are connected in parallel on a breadboard, with the wiring for one sensor shown in Figure 7.

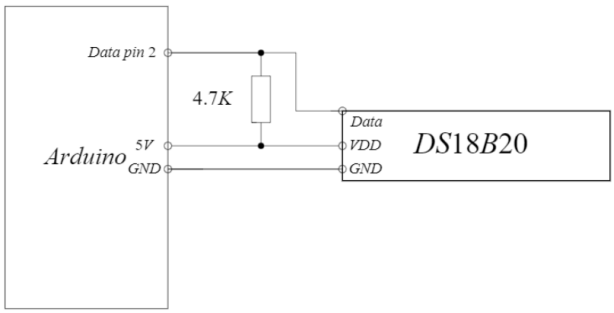

Figure 7: Wiring scheme Temperature sensor to Arduino

To regulate the aluminum block's temperature, the XH-W3001 temperature controller is connected between the adapter and the Peltier element, with a built-in temperature sensor mounted in the aluminum block (Figure 8). The controller maintains the desired temperature with an accuracy of 0.1°C, activating the Peltier element as needed. The temperature of the aluminium block will increase rapidly when turned on due to its high conductivity, the calculation for this can be seen in the report of Bart[4]. To control the temperature of the XH-W3001 a temperature range can be set for when the controller has to turn the Peltier element on and for when it has to turn of again. For the experiments the first set of tests where done with the Peltier element turning on immediately and turning of when reaching 45.0°C. The temperature will then overshoot a bit and cool down again. When the temperature of the aluminium block cools down to 49.9 the controller will turn the Peltier element on again. The Peltier element is on for an average of 6.5 seconds and then off for an average of 88 seconds. This results in a percentage of the Peltier element being on for 7.3% of the experiments. The second set of tests will have the temperature of the aluminum block controlled at 50°C

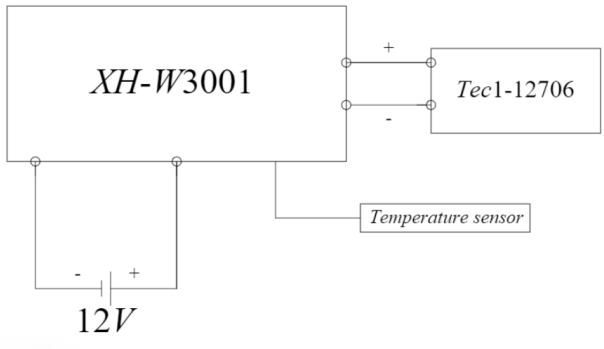

Figure 8: Wiring scheme XH-W3001 Temperature controller

2.3.1 Peltier Element

The TEC1-12706 Peltier module was chosen for its ability to transfer heat between its sides, offering a simple and reliable heat delivery method. It measures 40mm x 40mm x 3.8mm, operates at 12V, and has a 60W heating capacity and a maximum temperature of 65°C, suitable for the experiment. An aluminum heat sink on the cold side enhances cooling performance, and thermal paste ensures efficient heat transfer by filling microscopic gaps between the Peltier element and the heat sink, and between the Peltier element and the aluminum block.

2.3.2 Temperature Sensors

The DS18B20 sensors were selected for their accessibility and appropriate temperature range (-55 to 125°C), with an accuracy of 0.06°C. Four sensors were placed evenly to measure the temperature distribution accu-

rately. The positions of the sensors are:

Sensor	**Height (cm)**
Sensor 1	1.50
Sensor 2	3.23
Sensor 3	4.96
Sensor 4	6.70

Table 1: Position of Temperature Sensors

2.3.3 Adaptor/Temperature Controller

A 12V 5Amp adapter powers the setup, sufficient for the 60W Peltier element and temperature controller.

3 Numerical Model

The numerical model developed for this project aims to simulate the heat conduction through paraffin wax, leveraging both the theoretical framework and experimental setup described in previous sections. This model uses the finite element method (FEM) to approximate the temperature distribution over time, providing a means to validate the experimental data and gain deeper insights into the heat transfer characteristics of paraffin wax.

3.1 Model Setup

The physical properties of paraffin wax, along with the dimensions and initial conditions of the experimental setup, serve as the foundational parameters for the numerical model. Key parameters of the paraffin wax include:

- **Thermal conductivity (k):** 0.25 W/(m·K)
- **Density (ρ):** 900 kg/m^3
- **Specific heat capacity of (c):** 2100 J/(kg·K)

In this model, the aim is to analyze the heat transfer through a cylindrical tube. The primary objective is to understand the energy balance within the system and quantify the heat loss due to convection.

Figure 9 illustrates a segment of the tube with length dx. Heat enters the segment with heatflux $q(x)$ through A_1 and exit with heatflux $q(x + dx)$. Additionally, there is convective heat loss q_{conv} from the surface area A_2 from the tube

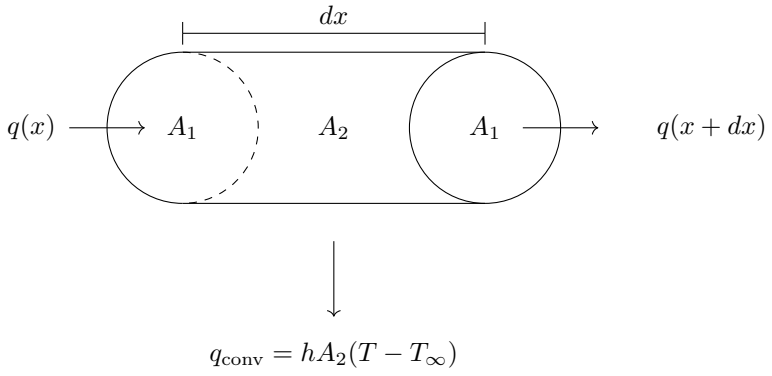

Figure 9: Energy balance across a differential element.

The model assumes one-dimensional heat conduction along the length of the paraffin wax cylinder. This gives the energy balance:

$$mc_p\frac{\partial T}{\partial t} = A_1q(x) - A_1q(x + dx) - hA_2(T - T_\infty) \tag{4}$$

$$m = \rho v : m = \rho\pi R^2 dx \tag{5}$$

$$A_1 = \pi R^2 \tag{6}$$

$$A_2 = 2\pi R dx \tag{7}$$

Substituting 5,6,7 in 4 gives:

$$\rho\pi R^2 dx c_p\frac{\partial T}{\partial t} = \pi R^2(q(x) - q(x + dx)) - 2\pi R h dx(T - T_\infty) \tag{8}$$

$$\rho c_p\frac{\partial T}{\partial t} = \frac{q(x) - q(x + dx)}{dx} - \frac{2h}{R}(T - T_\infty) \tag{9}$$

$$\frac{q(x) - q(x+dx)}{dx} = \frac{dq}{dx} \tag{10}$$

$$q = -k\frac{\partial T}{\partial x} \tag{11}$$

Substituting 10,11 in 9 gives:

$$\rho c_p \frac{\partial T}{\partial t} = k\frac{\partial^2 T}{\partial x^2} - \frac{2h}{R}(T - T_\infty) \tag{12}$$

For simplicity introduce θ, α and β:

$$\theta = T - T_\infty; \quad d\theta = dT; \quad d^2\theta = d^2T \tag{13}$$

$$\alpha = \frac{k}{\rho c} \tag{14}$$

$$\beta = -\frac{2h}{R\rho c} \tag{15}$$

simplifying the heat equation to:

$$\frac{\partial \theta(x,t)}{\partial t} = \alpha\frac{\partial^2 \theta(x,t)}{\partial x^2} + \beta\theta(x,t) \tag{16}$$

where α is the thermal diffusivity, and β is the heat loss term.

3.2 Boundary Conditions

In this model, two types of boundary conditions are used: a Dirichlet boundary condition at the left boundary and a Neumann (convective) boundary condition at the right boundary.

3.2.1 Dirichlet Boundary Condition

The Dirichlet boundary condition specifies a constant temperature at the left boundary of the paraffin wax. This boundary represents the heated end of the wax cylinder, where the temperature is maintained at a fixed value throughout the simulation.

$$T(0,t) = T_{\text{heat}} \tag{17}$$

The temperature at the left boundary (T_{heat}) is set to 39.52 °C for the first set of experiments, where the temperature of the aluminium block is controlled at 45°C. This value of 39.52 is a calculated value based on the temperature jump that exists between the aluminium block and the paraffin due to the thermal contact conductance. For the calculation look in the report of Bart[4]. This boundary condition ensures that heat is continuously supplied to the material, driving the conduction process.

3.2.2 Neumann (Convective) Boundary Condition

At the right boundary (x = L), a convective boundary condition is applied. This boundary condition models the heat exchange between the paraffin wax and the surrounding air, characterized by a convective heat transfer coefficient (h) and the ambient air temperature (T_∞).

The convective boundary condition is described by Newton's law of cooling:

$$-k\left.\frac{\partial T}{\partial x}\right|_{x=L} = h(T(L,t) - T_\infty) \tag{18}$$

Where:

- k is the thermal conductivity of paraffin wax.
- $\frac{\partial T}{\partial x}$ is the temperature gradient at the right boundary.
- h is the convective heat transfer coefficient.
- $T(L,t)$ is the temperature at the right boundary at time t.
- T_∞ is the ambient air temperature.

The convective heat transfer coefficient h is set to 1.7 W/(m^2·K) for the tests at 45°C and to 1.8 W/(m^2·K) for the tests at 50°C. The ambient air temperature T_∞ is 19.15 °C. This boundary condition captures the cooling effect of the surrounding air on the paraffin wax.

3.3 Numerical Implementation

The numerical solution involves the following steps:

1. **Discretization:** The domain is divided into 100 finite elements. The capacity matrix C and conductance matrix K are constructed based on the element connectivity and the thermal properties of paraffin wax.
2. **Initial Conditions:** The initial temperature distribution is set to a uniform value of $T_0 = 19.15$ °C, except at the heated boundary where T_{heat} is applied.
3. **Time Stepping:** The temperature distribution is updated at each time step using an implicit finite element method. The system of linear equations is solved iteratively to update the temperature at each node.
4. **Boundary Conditions:** At each time step, the boundary conditions are enforced by modifying the matrix equations accordingly. The convective boundary condition at the right edge is incorporated into the matrix formulation.

3.4 Simulation Execution

The simulation runs for a total time of 42082 seconds, with a time step of 1.9 seconds, because the Arduino collects the data from the sensors only after 1.9 seconds. At each time step, the temperature at four sensor positions (corresponding to the experimental setup) is recorded.

In Figure 10 the temperature distribution along the spatial domain at each hour can be seen. It shows that the simulation reaches steady state.

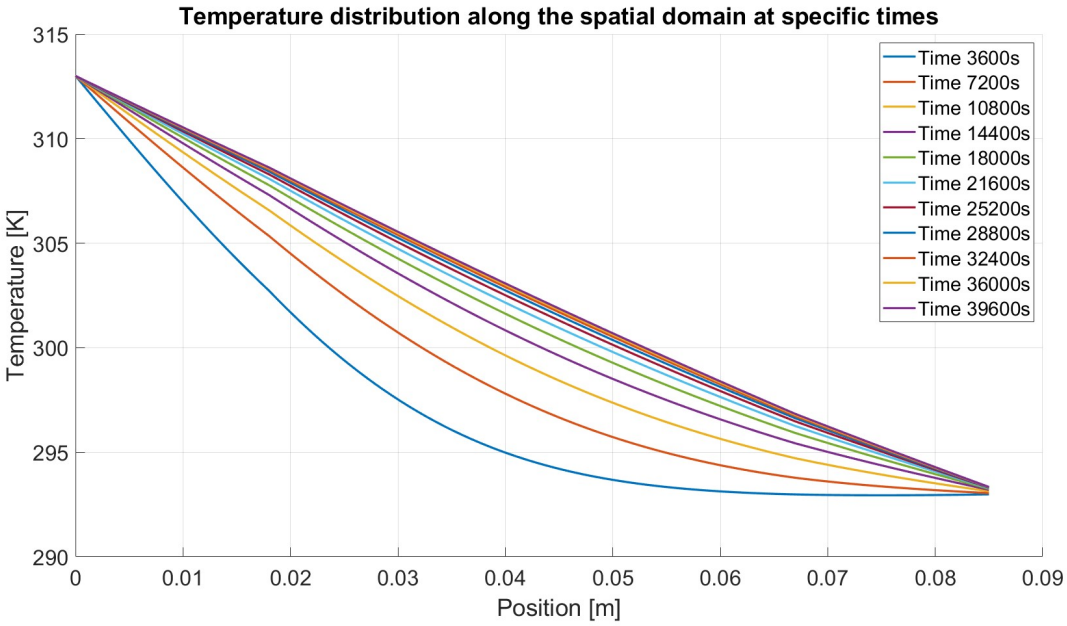

Figure 10: Temperature distribution along the spatial domain at each hour

4 Comparison to the experiment

The results from the numerical model are compared with the experimental data to evaluate the model's accuracy and the thermal properties of paraffin wax.

4.1 Temperature Distribution

The temperature distribution over time, as predicted by the numerical model, is plotted alongside the experimental data from the four sensors. Figure 11 shows the temperature profiles at the four sensor locations, with solid lines representing the numerical estimates and dashed lines representing the experimental measurements, with the controlled temperature at 45°C. Figure 12

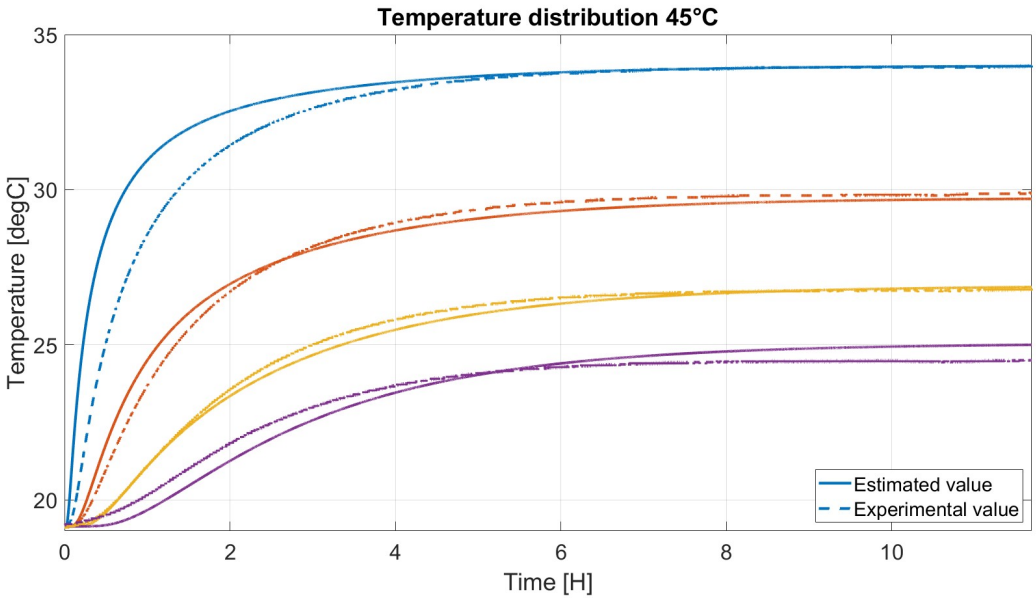

Figure 11: Model vs Experimental data at 45°C

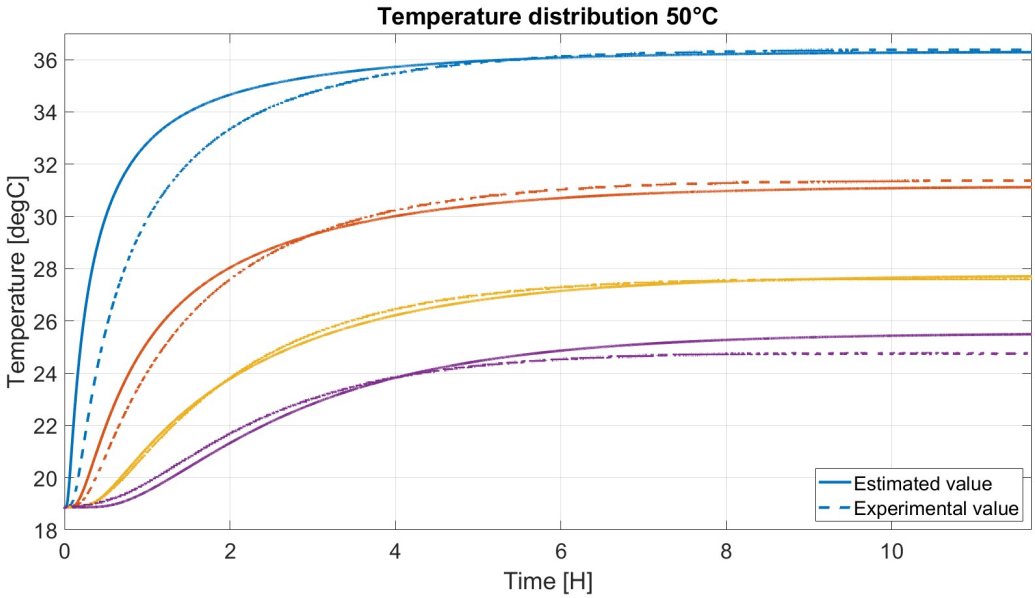

Figure 12: Model vs Experimental data at 50°C

The comparison between the numerical and experimental results reveals several key observations:

- **Accuracy of the Numerical Model:** The numerical model demonstrates good agreement with the experimental data, particularly in the steady state phase of the experiment. The model accurately captures the temperature rise at all sensor positions, indicating that the thermal properties used in the model are reasonable approximations.
- **Discrepancies:** Minor discrepancies between the model and experimental data can be observed, especially at early times. These discrepancies could be attributed to several factors, including:
  - Variations in material properties (e.g., the thermal conductivity of the paraffin wax may not be perfectly constant).
  - Experimental errors such as sensor calibration issues or the exact position of the sensors.
  - Simplifications in the model, such as assuming one-dimensional heat conduction.
- **Heat Transfer Dynamics:** The results highlight the temperature-dependent nature of paraffin wax's thermal conductivity. The experimental data shows slight deviations from the model predictions, particularly at higher temperatures, suggesting that thermal conductivity may vary with temperature.
- **Sensor Performance:** The placement and accuracy of the temperature sensors are validated through the close match with the model predictions. The data from sensors 1 and 2 (closer to the heated end) exhibit a more rapid temperature rise compared to sensors 3 and 4, consistent with the expected heat diffusion behavior.

4.2 Improvements and Future Work

To enhance the accuracy and reliability of the numerical model, the following improvements can be considered:

- **Refinement of Material Properties:** Conducting additional experiments to measure the temperature dependence of thermal conductivity for paraffin wax would provide more precise input for the model. Detailed measurements of specific heat capacity and density across different temperature ranges would also improve the model's accuracy.
- **Incorporation of Multidimensional Effects:** Although the one-dimensional assumption simplifies the problem, incorporating two-dimensional or three-dimensional effects could improve model accuracy, especially for larger diameters. This would involve more complex numerical formulations but could provide a more realistic representation of heat transfer.
- **Enhanced Boundary Conditions:** Including more detailed boundary conditions, such as varying convective heat transfer coefficients or accounting for heat losses through insulation, could further refine the model. Additionally, considering the effects of radiation heat transfer could enhance the boundary condition accuracy.
- **Validation with Different Setups:** Testing the model with different experimental setups, including varying the dimensions of the paraffin wax and the heating conditions, would help validate its general applicability. This could involve different heating sources, varied ambient temperatures, and different sensor placements.

5 Conclusion

In this study, the thermal conductivity of paraffin wax was investigated through both experimental and numerical methods. The main goal was to create a dependable experimental setup to measure the heat conduction of paraffin wax and to analyze these results with a numerical model.

The experimental setup was carefully designed and optimized based on an initial prototype. These experimental findings were then compared to a numerical model, which utilized the finite element method to simulate heat conduction.

The numerical model demonstrated a close alignment with the experimental data in terms of temperature behavior. However, discrepancies were observed, especially during the initial temperature rise phase. The numerical model included heat loss considerations, but these losses had a greater impact at the start of the experiment in practice than the model predicted. The most significant steady-state deviation was noted in sensor 4, with sensor 1 showing the highest temperature losses, while sensor 3 provided the most accurate readings.

Despite these differences, the steady-state temperatures and overall trends were well-matched between the model and the experimental data, affirming the numerical model's validity for simulating heat conduction in paraffin wax. These results highlight the importance of accounting for initial conditions and heat loss effects in thermal conductivity research.

In summary, this project successfully developed an experimental setup and validated a numerical model for investigating the thermal conductivity of paraffin wax, though further improvements are necessary. Future research should aim to refine the model to different scales and adding two-dimensional or three-dimensional effects. This could improve the model accuracy.

To further improve the experimental setup accuracy and reliability, several enhancements can be made. One significant improvement is the use of smaller temperature sensors. The current sensors measure over a height of 6mm, leading to a measurement range of +/- 3mm, which is relatively large for a setup with an overall height of 85mm. Utilizing smaller sensors would yield more precise temperature measurements, thereby increasing the experiment's overall accuracy.

Additionally, adding an extra temperature sensor closer to the heating surface would be beneficial. The current first sensor is positioned 18mm away from the heating surface, which is quite distant. Positioning an additional sensor closer to the heating surface would provide more accurate data for the initial temperature gradient, aiding in a better understanding of early-stage heat conduction behavior. These improvements would significantly enhance the experimental setup and provide more reliable data for future studies.

References

[1] Lia, Y. (2022). Experimental study on preparation and thermal storage properties of expanded graphite/-paraffin wax as a shape-stabilized phase change material.
[2] Wikipedia. (2024a). Thermal conduction. https://en.wikipedia.org/wiki/Thermal_conduction
[3] Wikipedia. (2024b). Heat equation. https://en.wikipedia.org/wiki/Heat_equation
[4] Meulendijks, B. (2024). Design of a paraffin wax heat conduction experiment.

6 Appendix A

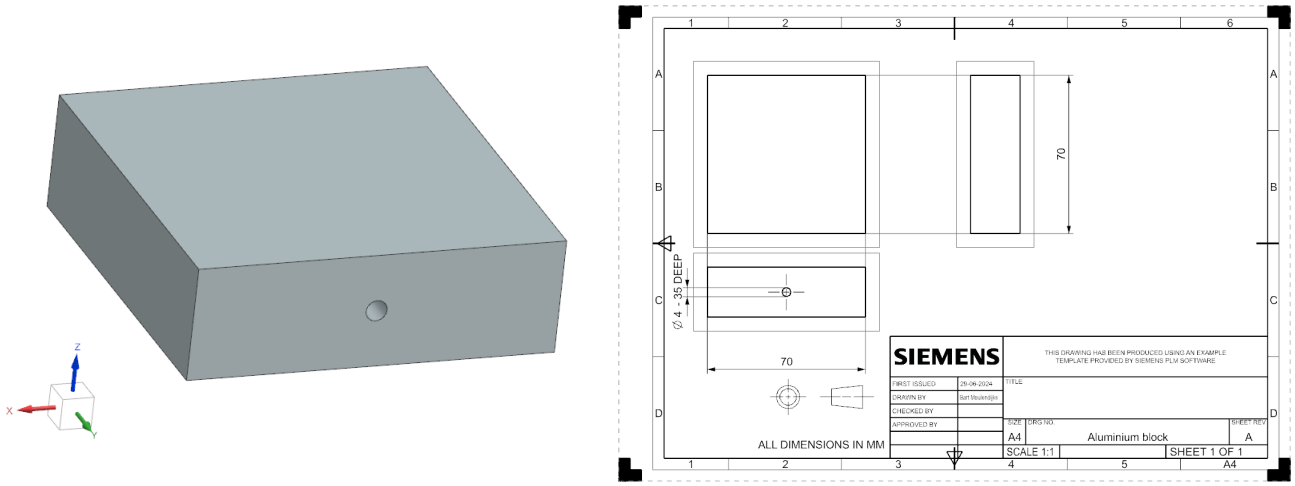

Figure 13: Aluminum block

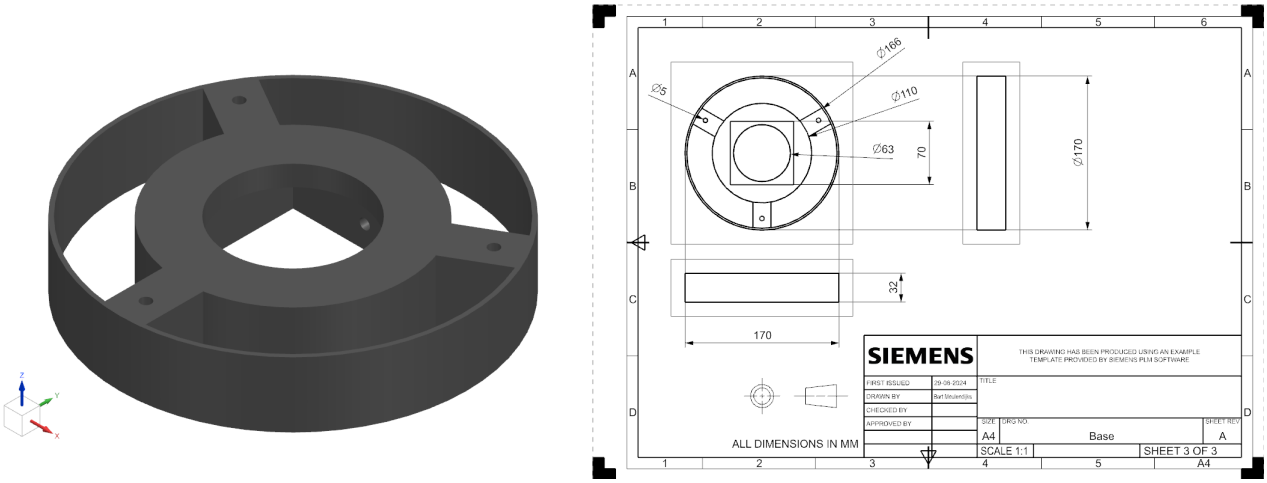

Figure 14: Casing base

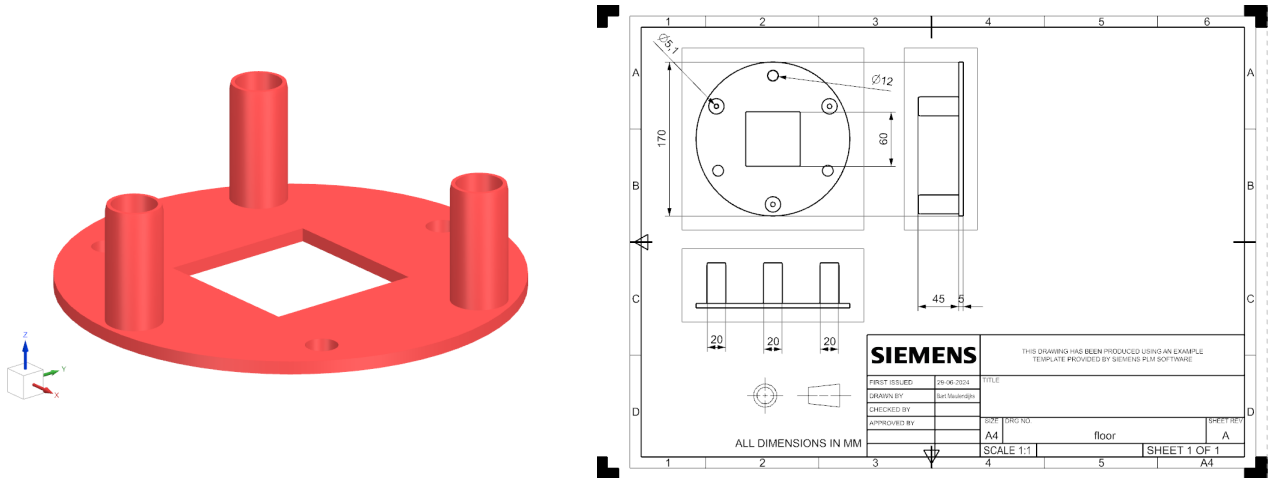

Figure 15: Casing Floor

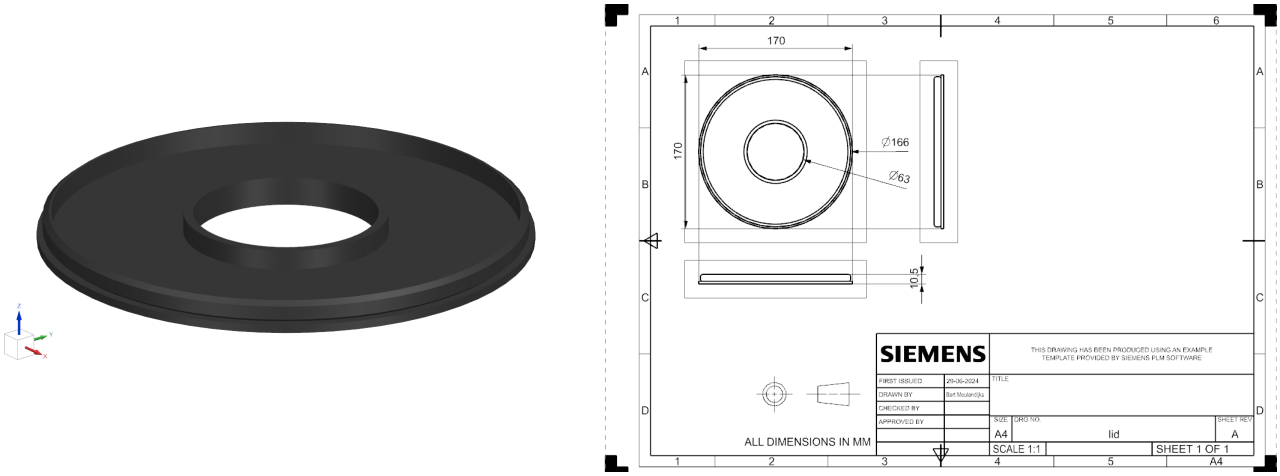

Figure 16: Casing Lid

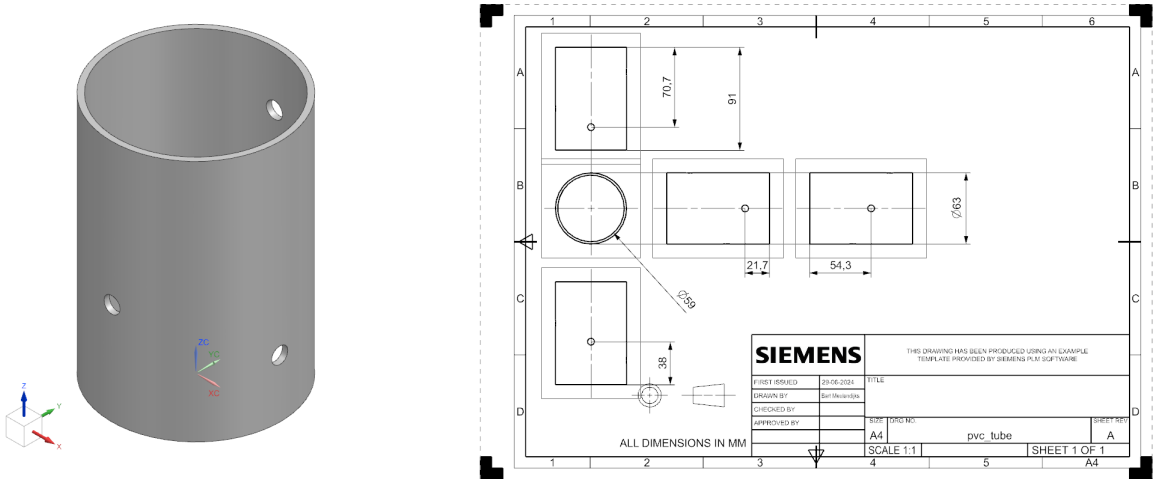

Figure 17: PVC Tube

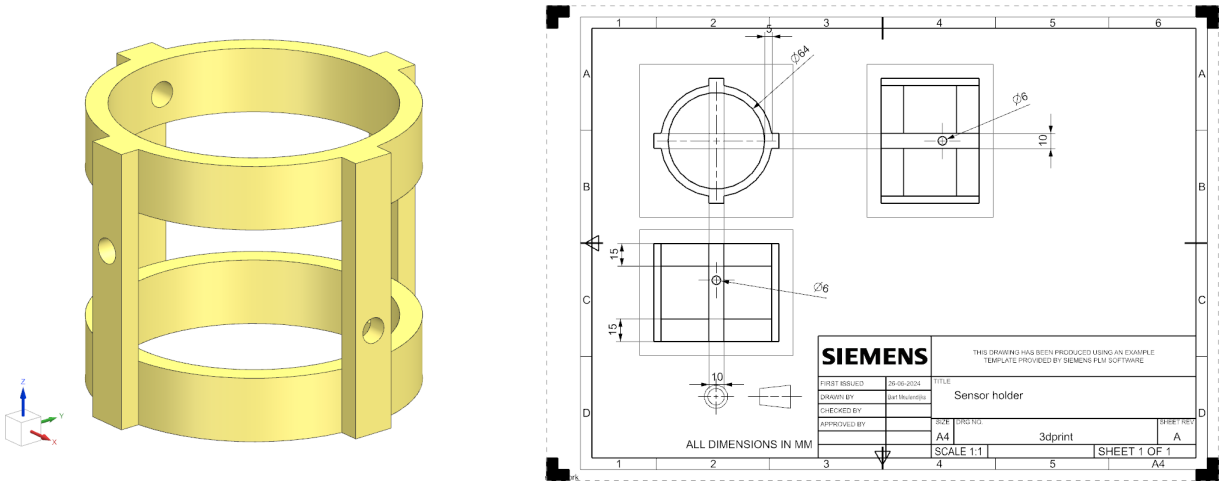

Figure 18: Sensor holder

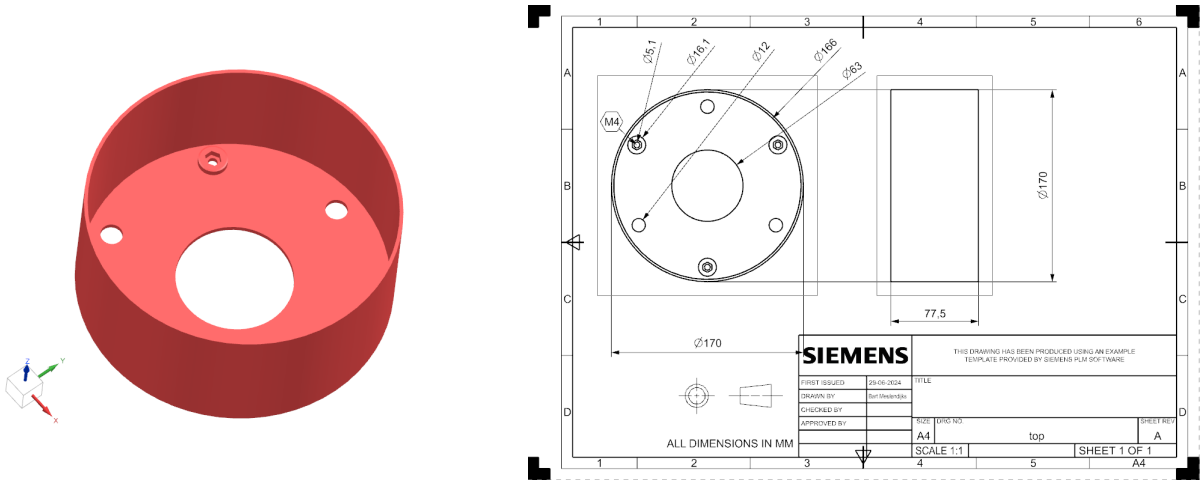

Figure 19: Casing Top

7 Appendix B

Reading data from the arduino

```
clear, close all, clc;
%% txt file
fileName = 'serialData.txt';    % enter name of file to write data to

fileID = fopen(fileName,'w');
%% setup serial port
port = 'COM4';                  % set serial port where the arduino is connected (e.g. 'COM4' on
    Windows or '/dev/cu.usbmodem11101' on Mac OSX)
baudRate = 9600;                % set baud rate to the same value as in the arduino script

s = serialport(port,baudRate);
%% GUI
figure('Position',[500,500,170,200]);
StopButtonHandle = uicontrol(   'Style', 'PushButton', ...
                                'String', 'Stop', ...
                                'Callback', 'delete(gcbf)',...
                                'Position',[20,20,120,40]);

uicontrol(   'Style', 'text', ...
             'String', "reading data from serial port "+port, ...
             'Position',[20,100,120,40]);
%% read serial data and write to text file
while true
  SerialData = readline(s);
  fprintf(fileID,SerialData);

  if ~ishandle(StopButtonHandle)
      disp('reading serial data stopped by user');
      break;
  end
end

fclose(fileID);

disp("serial data written to "+fileName)
```

Numerical model Heat conduction

```
close all; clear; clc;

% Load data
data = load('Complete50_1.txt');
data1 = data(:, 4);
data2 = data(:, 1);
data3 = data(:, 3);
data4 = data(:, 2);

% Physical properties of paraffin wax
k = 0.25;    % thermal conductivity [W / (m K)]
rho = 900;  % density [kg / m^3]
cp = 2100;  % specific heat [J / (kg K)]

% Parameters for initial and boundary conditions
T_heat = 43.04;   % constant temperature at the left edge [degC] 45=39.52, 50 = 43.04
T0 = 18.87;       % initial temperature [degC] 45= 19.15, 50 = 18.87
T_inf = 18.87;    % air temperature [degC] 45= 19.15, 50 = 18.87
h = 1.8;      % heat transfer coefficient [W / (m^2 K)] 45 =1.7, 50= 1.8

% Define transformed temperatures
theta_heat = T_heat - T_inf;
theta0 = T0 - T_inf;

% Define dimensions [m]
L = 8.5e-2;     % length
R = 29.5e-3;    % radius

% Define position of the sensors [m]
```

```
sensors = [1.5e-2; 3.23333e-2; 4.96666e-2; 6.7e-2];

% Define numerical domain
ne = 100;       % number of elements
np = ne + 1;    % number of points
domain = linspace(0, L, np)';
dx = domain(ne + 1) - domain(ne);

% Define indexes to store temperature
indexes = zeros(4, 1);
for i = 1 : 4
    [~, indexes(i)] = min(abs(domain - sensors(i)));
end

% Define time domain [s]
t = 42082;   % final time
dt = 2.0;       % time step
t_vec = (dt : dt : t)';

% Define number of measurements
n_meas = t / dt;

% Define alpha and beta
alpha = k / (rho * cp);
beta = - 2 * h / (R * rho * cp);

% Define connectivity matrix
IEN = zeros(ne, 2);
for i = 1 : ne
    IEN(i, 1) = i;
    IEN(i, 2) = i + 1;
end

% Define capacity matrix C
C = zeros(np, np);
for e = 1 : ne
    c_e = dx / 6 * [2, 1;
                    1, 2];
    for ilocal = 1 : 2
        iglobal = IEN(e, ilocal);
        for jlocal = 1 : 2
            jglobal = IEN(e, jlocal);
            C(iglobal, jglobal) = C(iglobal, jglobal) + c_e(ilocal, jlocal);
        end
    end
end

% Define initial temperature
theta = theta0 * ones(np, 1);
theta(1) = theta_heat;

% Loop
theta_store = zeros(n_meas, 4);
for i = 1 : n_meas

    % Define conductance matrix K
    K = zeros(np, np);
    for e = 1 : ne
        k_e = 1 / dx * [1, -1;
                        -1,  1];
        for ilocal = 1 : 2
            iglobal = IEN(e, ilocal);
            for jlocal = 1 : 2
                jglobal = IEN(e, jlocal);
                K(iglobal, jglobal) = K(iglobal, jglobal) + k_e(ilocal, jlocal);
            end
        end
    end

    % Define matrix A
```

```
    A = C / dt + alpha * K - beta * C;

    % Define vector b
    b = C / dt * theta;

    % Apply boundary condition at X = 0
    A(1, :) = 0;
    A(1, 1) = 1;
    b(1) = theta_heat;

    % Apply boundary condition at X = 1
    A(end) = A(end) + h / (rho * cp);

    % Solve linear system
    theta = A \ b;

    % Store values of theta
    for j = 1 : 4
        theta_store(i, j) = theta(indexes(j));
    end
end

% Define vector with temperatures
T1 = theta_store(:, 1) + T_inf;
T2 = theta_store(:, 2) + T_inf;
T3 = theta_store(:, 3) + T_inf;
T4 = theta_store(:, 4) + T_inf;
hour = 3600;
% Plot
figure;
plot(t_vec/ hour, T1, 'Color', "#0072BD", 'LineWidth', 2.5);
hold on;
plot(t_vec/ hour, T2, 'Color', "#D95319", 'LineWidth', 2.5);
hold on;
plot(t_vec/ hour, T3, 'Color', "#EDB120", 'LineWidth', 2.5);
hold on;
plot(t_vec /hour, T4, 'Color',"#7E2F8E", 'LineWidth', 2.5);
hold on;
plot(t_vec/ hour, data1, 'Color', "#0072BD", 'LineWidth', 2.5,'LineStyle','--');
hold on;
plot(t_vec/ hour, data2, 'Color', "#D95319", 'LineWidth', 2.5,'LineStyle','--');
hold on;
plot(t_vec/ hour, data3, 'Color', "#EDB120", 'LineWidth', 2.5,'LineStyle','--');
hold on;
plot(t_vec/ hour, data4, 'Color',"#7E2F8E", 'LineWidth', 2.5,'LineStyle','--');
grid on;
xlabel('Time [H]');
ylabel('Temperature [degC]');
xlim([0 max(t_vec/hour)]);
ylim([18 37]);
legend('Estimated value', '', '', '', ...
    'Experimental value', '', '', '');
legend('Location','southeast')
title('Temperature distribution 50 C ');
set(gca, 'FontSize', 20);
```